

# Performance Analysis of an integrated Semi-Transparent Thin Film PV Vacuum Insulated Glazing

Hasila Jarimi<sup>1</sup> , Ke Qu<sup>1</sup>, Shihao Zhang<sup>1</sup>, Qinghua Lv<sup>1,2</sup>, Daniel Cooper<sup>1</sup>, Yuehong Su<sup>1</sup>, Saffa Riffat<sup>1</sup>

<sup>1</sup>Nottingham University, Architecture and Built Environment, Nottingham, United Kingdom

<sup>2</sup>Hubei University of Technology, Environmental Hubei Collaborative Innovation Center for High-efficient Utilization of Solar Energy, Hubei, Wuhan, China

## ABSTRACT

This paper is intended to design and develop a thermal model of an integrated semi-transparent thin-film PV vacuum glazing with four layers of glass called PV VG-4L. The design of the glazing involves integration between a thin-film PV glazing with a double vacuum glazing (both manufactured independently), and an additional layer of self-cleaning coated glass. For the mathematical model, the energy balance equations were derived for the thin-film PV glass, the glass panes of the vacuum glazing and the edges of the internal and external glass surfaces (facing indoors and outdoors respectively). The model was numerically solved in MATLAB. To evaluate the performance of the PV VG-4L, the prototype was manufactured and investigated at lab-scale and also under real conditions. At lab-scale, experiments were conducted at steady-state conditions using a TEC driven calibrated hot box at Sustainable Energy Research Lab, University of Nottingham, UK. Meanwhile, outdoors, the prototype was tested at a research house at the University of Nottingham, UK. The developed model was then validated against the experimental results by direct comparison on the trend of the experimental and theoretical curves obtained, and also by conducting error analysis using root mean squared percentage deviation (RMSPD) method. When tested using the calibrated hot box, by following closely the ISO 12567 standards, the average measured total U-value is 0.6 W/m<sup>2</sup>K. From the analysis, the computed RMSPD value for the glazing surface temperature and the U-value are 4.75 % and 0.96% respectively. The RMSPD computed for the glazing surface temperatures, electrical power generated under real conditions and U-value are 2.58 %, 1.4% and 6.86 % respectively. The theoretical and experimental results are concluded to be in good agreement. The thermal and electrical performance of a building retrofitted with and without PV VG-4L was examined and discussed. At building efficiency level, the PV VG-4L not only can produce power, but it also has high insulating properties. The promising U-value implies that the glazing's range of potential applications can be improved depending on the energy needs and applications, which includes its use in BIPV solar façades (PV curtain walling) for commercial buildings, greenhouses, skylights and conservatories.

### Keywords:

Semi-transparent thin-film PV; Low U-value; SHGC.

## INTRODUCTION

There is a continuous growth in global buildings sector reaching an estimated 235 billion m<sup>2</sup> in 2016. Building energy consumption was reported to account for 28% of global energy-related CO<sub>2</sub> emissions in 2018. It has also been reported that, in that year, buildings-related CO<sub>2</sub> emissions rise to as high as 9.6 Gt CO<sub>2</sub> for the second year in a row [1]. In terms of efficient building sector, there is a great potential for building-integrated PV technologies (BIPV) to offer potential energy savings of a building by gener-

ating solar energy resources captured via the building materials itself. This is portrayed by the global BIPV market which is estimated to reach revenues of around \$7 billion by 2024, growing at a CAGR of approximately 15% during 2018-2024 [2].

A thin-film photovoltaic (PV) glass is a clean energy technology that uses transparent photovoltaic cells such as amorphous silicon ( $\alpha$ -Si) and microcrystalline/amorphous ( $\mu$ C-Si) to harvest solar energy. These pho-

### Article History:

Received: 2019/10/08

Accepted: 2019/10/31

Online: 2019/12/31

**Correspondence to:** Hasila Jarimi,  
Nottingham University, Department of  
Architecture and Built Environment,  
School of Engineering, United Kingdom

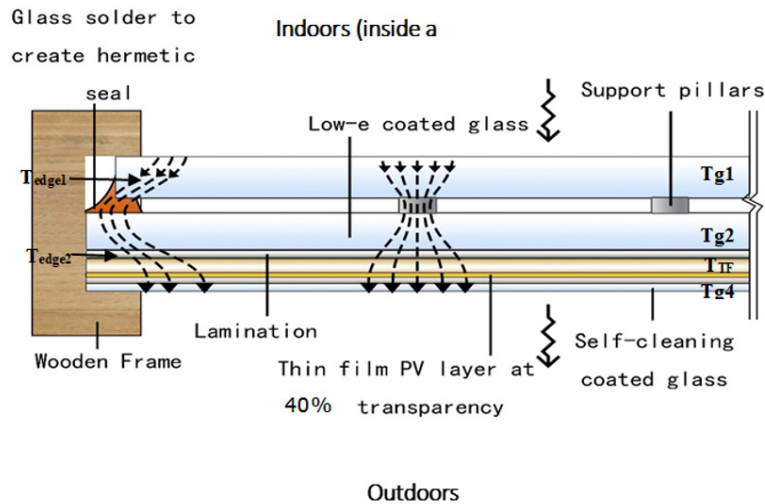


**Figure 1.** Schematics of PV VG-4L and the heat flow through the glass panes.

Photovoltaic cells are typically deposited on super-clear float glass, with TCO layers as the conductive layers and an ultra-clear float glass as the glass cover. When replacing a building envelope, in the context of building insulation performance which is mainly represented by the U-value, thin-film PV glass has a similar thermal transmittance (U-value) to single glazing ( $\sim 5 \text{ W/m}^2\text{K}$ ) [3]. Therefore, to improve its thermal performance, thin-film PV glass is generally integrated into double glazing applications [4]. However, such configurations have certain limitations, including the heavy weight due to the thick frame, while the use of the inert gas between the glass panes is not easy to maintain. A group of researchers from China [5] proposed an integration between a thin-film PV glazing with a vacuum glazing. The glazing prototype was designed and manufactured in such a way that a lamination layer was sandwiched between the thin film PV glazing unit and a vacuum glazing unit, both are independently manufactured. According to the researchers, although semi-transparent photovoltaic windows can generate electricity in situ, they also increase the cooling load of buildings significantly due to the waste heat as a by-product. Experiment has been conducted and the results have indicated that the prototype can not only generate electricity, but also help reduce the cooling load as well as improve the indoor thermal comfort. Recently, researchers [6] investigated a combined semi-transparent multicrystalline PV vacuum glazing. They have found that the combination of multicrystalline PV cells with vacuum glazing provide low overall heat transfer coefficient, reduces solar heat gain, generates clean electricity and allows comfortable daylight. In this paper, a novel design of semi-transparent thin-film PV glazing integrated with a vacuum glazing and a layer of self-cleaning coated glass called PV-VG 4L is introduced. Setting it apart from the research conducted by the researchers mentioned above, this paper is intended to develop the thermal model and also to discuss the performance analysis of the novel glazing design in detail both in the lab and real conditions.

Using the validated mathematical model, a building thermal load retrofitted with PV VG-4L in winter condition in the UK was examined.

## DESIGN CONCEPT AND HEAT TRANSFER ANALYSIS OF THIN FILM PV VACUUM INSULATED GLAZING (PV VG-4L)

The design of PV VG-4L is illustrated in Figure 1. PV VG-4L involves an integration between a thin film PV glazing with a double vacuum glazing (both manufactured independently) and an additional layer of self-cleaning coated glass which totaling 4 layers of glass units which gives the total thickness of 14 mm. The use of self-cleaning coating on the glass surface will increase PV life time, enhance efficiency by 1-3%, and reduce cleaning requirements. The layers were combined via Ethylene Vinyl Acetate (EVA) film using an autoclave facility which was set at its optimum temperature and pressure. For this research, a-Si thin film PV glazing (40% transparency) was used. The heat transfer was analysed based on the following temperature nodes which are; the average glass temperature facing indoors denoted by  $T_{g1}$ , the average internal glass temperature denoted by  $T_{g2}$ , the average temperature of the thin film PV glass denoted by  $T_{TF}$  and the average temperature of the self-cleaning coated glass denoted by  $T_{g4}$ . The lateral heat transfer ends at the point right at the edge sealing and the temperature was denoted as  $T_{edge1}$ . Due to high thermal conductivity of the edge sealing, it acts as a short circuit for the heat transfer at the edges of the glazing. Meanwhile, due to high thermal conductivity between  $g2$  and  $g4$ , the lateral heat conduction in the glass slab  $g2$  and thin film PV glass (TF) are assumed negligible. The temperature of the position in  $g4$ , of which the edge heat transfer takes place is denoted as  $T_{edge1}$ .

ted as  $T_{edge2}$ . For the uninsulated edges, there will be heat transferred from the internal ambient to the area around the edges.

When the PV panel absorbed solar radiation, a fraction of the absorbed solar radiation will be converted into useful power meanwhile a fraction will be wasted in the form of heat. This heat released by the PV panel is insulated from the building via the vacuum layer of which, the main heat transfer occurs in the gap are mainly due to radiation and conduction through the support pillars and the edge seal. In the summer, this can be considered as an advantage since the installation of PV glazing would normally cause additional heating during summer of which in return, increase the cooling load of a building. Based on the heat transfer mechanism, the energy balance equations at steady state conditions were developed. In order to simplify the analysis, the following assumptions have been made:

- The heat transfer involved is assumed symmetrical. Therefore, we only consider a quarter of the PV VG-4L area in the heat transfer analysis.
- In this study, we have considered the lateral heat transfer through the glass slab in g1 and g4. This is because, the vacuum glazing is highly thermally insulated which makes the lateral heat transfer to become prominent.
- The edge boundaries of the PV VG-4L are well insulated and hence the edge losses are assumed negligible.
- Due to high thermal conductivity of the edge sealing, the edge seal is assumed as a thermal short circuit.
- Meanwhile, due to high thermal conductivity between g2 and g4, the lateral heat conduction in the glass slab g2 and thin-film PV glass (TF) are assumed negligible.
- Multireflection between the inner glass panes are considered in the calculation of the absorbed solar radiation by the glass layers.

To simulate the performance of the PV VG-4L, energy balance equations were developed for each of the temperature nodes.

**For g1:**

$$\underbrace{S_{g1}}_1 + \underbrace{h_{a\_g1}(T_{a\_i} - T_{g1})}_2 = \underbrace{h_{g1\_g2}(T_{g1} - T_{g2})}_3 + \underbrace{h_{k\_edge}(T_{g1} - T_{edge1})}_4 \quad (1)$$

The heat transfer terms are defined as follows:

- 1: The rate of the solar energy received by the glass cover or surface facing indoors after transmission through different glass layers per unit area; 2: The rate of heat transfer from the indoor ambient to g1 per unit area; 3: The rate of heat transfer from g1 to g2 per unit area. The heat transfer includes heat conduction through the glass slabs of g1, followed by heat transfer in the vacuum gap (due to the heat conduction of the gas particles) radiative heat transfer, and heat conduction through the support pillars; 4: The rate of lateral heat conducted along the x-direction and y-direction of the PV VG-4L from the centre of the PV VG-4L.

**For Tedge1:**

$$\underbrace{h_{k\_edge}\gamma_c(T_{g1} - T_{edge1})}_4 + \underbrace{h_{ice\,edge}\gamma_{edge}(T_{a\_i} - T_{edge1})}_5 = \underbrace{h_{edge}\gamma_{edge}(T_{edge1} - T_{edge2})}_6 \quad (2)$$

The heat transfer terms are defined as follows:

- 5: The rate of heat transfer from the indoor ambient to the edge area per unit glazing area (if not insulated); 6: The rate of heat transfer from edge 1 to edge 2 through g2, TF and EVA layer per unit area.

**For g2:**

$$\underbrace{h_{g1\_g2}(T_{g1} - T_{g2})}_3 + \underbrace{S_{g2}}_7 = \underbrace{h_{g2\_TF}(T_{g2} - T_{TF})}_8 \quad (3)$$

The heat transfer terms are defined as follows:

- 7: The rate of the solar energy received by g2 after transmission through different glass layers per unit area; 8: The rate of heat transfer from g2 to TF through the EVA layer per unit area.

**For TF:**

$$\underbrace{h_{g2\_TF}(T_{g2} - T_{TF})}_8 + \underbrace{S_{TF}}_9 = \underbrace{h_{TF\_g4}(T_{TF} - T_{g4})}_{10} \quad (4)$$

The heat transfer terms are defined as follows:

- 9: The rate of the solar energy received by thin film PV layer (TF) after transmission through different glass layers per unit area; 10: The rate of heat transfer from TF to g4 through the EVA layer per unit area.

**For Tedge2:**

$$\underbrace{h_{edge}\gamma_{edge}(T_{edge1} - T_{edge2})}_6 = \underbrace{h_{k\_edge}\gamma_c(T_{edge2} - T_{g4})}_{11} \quad (5)$$

**Table 1.** The definition of the symbol used.

Symbol	Definition	Symbol	Definition
$S_{g1}, S_{g2}, S_{TF}$	The absorbed solar radiation for $g1$ , $g2$ and $TF$ respectively	$\gamma_c$	Correction factor due to the total area of the PV VG-4L
$\gamma_{edge}$	Correction factor due to the total area of edge sealing	$h_{edge}$	Conductive heat transfer coefficient due to the edge sealing
$\delta_{edge}$	The edge sealing thickness	$h_{iedge}$	Total heat transfer coefficient from the indoor ambient air to the uninsulated edge sealing area
$h_p$	Heat transfer coefficient through the support pillars	$h_{g1\_g2}$	The total heat transfer coefficient from $g1$ to $g2$ of vacuum glazing
$h_{k\_edge}$	The lateral heat transfer to the glass edge	$h_{g2\_TF}$	The total coefficient of heat transfer by conduction from $g2$ to the thin film PV glass layer $TF$ .
$h_{a\_g1}$	Total heat transfer coefficient from the internal ambient to $g1$	$k_{edge}$	Thermal conductivity through the edge sealing
$h_{TF\_g4}$	The total heat transfer coefficient by conduction from the thin film PV glass layer $TF$ to $g4$ .	$T_{a\_i}$	Indoor ambient temperature
$h_o$	Total heat transfer coefficient from the external glass $g4$ to the ambient	$T_{a\_o}$	Outdoor ambient temperature

The heat transfer terms are defined as follows:

11: The rate of lateral heat conduction along the x-direction and y-direction of the PV VG-4L from the centre of the PV VG-4L.

For  $\gamma_c$ :

$$\frac{h_{TF\_g4}(T_{TF} - T_{g4})}{10} + \frac{h_{k\_edge} \gamma_c (T_{edge2} - T_{g4})}{11} + \frac{S_{g4}}{12} = \frac{h_o (T_{g4} - T_{a\_o})}{14} \quad (6)$$

The heat transfer terms are defined as follows:

12: The rate of the solar energy received by  $g4$  after transmission through different glass layers per unit area; 14: The rate of heat transfer from  $g4$  to  $T_{a\_o}$  per unit area.

To theoretically predict the glazing's electrical performance, the following correlation developed by Schott [7] and Evans [8] is used:

$$\eta_{eff} = \eta_{Tref} (1 - \beta_{ref} (T_{TF} - T_{ref})) \quad (7)$$

Where  $\beta_{ref}$  temperature coefficient of the thin-film PV is cells and  $\eta_{Tref}$  is the electrical efficiency at reference temperature (25°C). From the simulation, the values of the average temperature of the glass sheets (layers) were used to compute the heat transfer coefficients summarised in Table A.1. The centre thermal resistance  $R_{centre}$  and the edge thermal resistance  $R_{edge\_tot}$  can be computed as in equation (8) and (9) respectively.

$$R_{centre} = \frac{1}{h_{a\_g1}} + \frac{1}{h_{g1\_g2}} + \frac{1}{h_{g2\_TF}} + \frac{1}{h_{TF\_g4}} + \frac{1}{h_o} \quad (8)$$

$$R_{edge\_tot} = \frac{1}{h_{edge}} + \frac{1}{h_{k\_edge}} + \frac{1}{h_{iedge}} \quad (9)$$

U-value is defined as the measure of heat transfer or thermal transmittance from a warm space of a building to the external cooler environment or vice versa. It reflects how well a glazing unit as a heat insulator. In this study, the centre U-value ( $U_{centre}$ ) and the total U-value ( $U_{total}$ ) may be computed using equation 10 and 11 respectively:

$$U_{centre} = \frac{1}{R_{centre}} \quad (10)$$

$$U_{total} = U_{centre} \gamma_c + u_{edge\_tot} \gamma_{edge} \quad (11)$$

In this study, to solve the energy balance equations, we have used the inverse matrix method. MATLAB is used to carry out the iteration process with Newton-Raphson iteration technique is used to estimate the temperature and hence the temperature-dependent heat transfer coefficients of the variables.

## RESULTS AND DISCUSSIONS

### U-Value Measurement using A TEC Driven Calibrated Hot Box

A PV VG-4L prototype as shown in Fig. 2 was manufactured. The U-value of the prototype was evaluated using the TEC-driven calibrated hot box built at the University of Nottingham. Interested readers may refer to [9] for



Figure 2. The PV VG-4L prototype



Figure 3. The calibrated hot box with the installed sample

further details. As can be seen in Figure 3, by following closely ISO 12567 standards, the sample was installed at the specimen area of the calibrated hot box. It was tested under three different air temperature conditions summarised in Table 2. However, the air speed in the hot and cold side were fixed at 0.3 m/s and 1.5 m/s respectively. Using the calibrated hot box, we could estimate the total heat transfer coefficient from the hot and cold surface of the PV VG-4L prototype. The values were then used as the input parameters for the computer simulation. To derive the absolute error, the Kline–McClintock second power law as given in NCEES (National Council of Examiners for Engineering and Surveying) (2001) is used. These errors were represented by the error bars of the associated curves. Additionally, the guideline in ISO 12567 was also being referred to evaluate the error from indoor testing.

The mathematical model validation method is performed by comparing the results obtained experimentally and theoretically based on the trends shown on the related graphs. In this study, the mathematical model has been validated against the indoor experimental data with the input parameters recorded in the experiment were used in the computer simulation for all the three different conditions. In addition to the direct comparison between the simulation and theoretical curves, the validation of the mathematical model is further justified using root mean square percentage deviation (RMSPD). As shown in Figure 4, and summarised in Table 3, the evaluated glazing surface temperatures and U-value are found to be in good agreement such that the trend of the theoretical curves are consistent with the experimental curves and the computed RMSPD for the temperatures and U-value are 4.75% and 0.96% respectively.

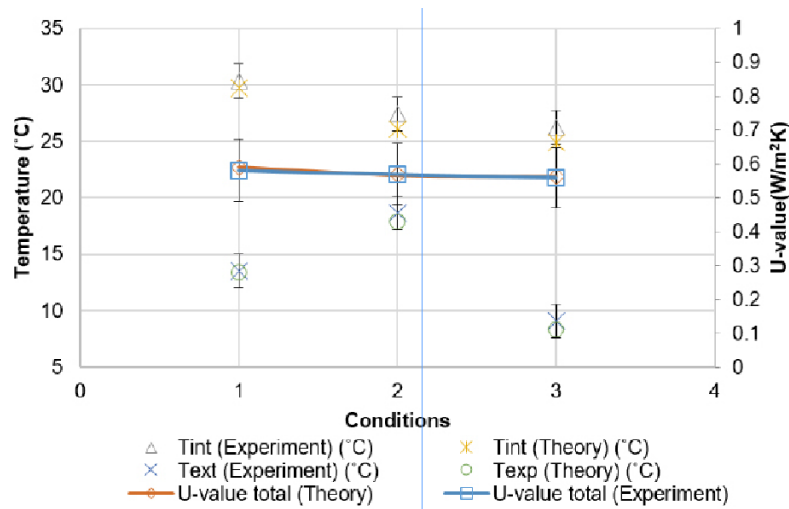


Figure 4. Comparison between the theoretical and experimental results for the glazing surface temperature and U-value using the calibrated hot box.

Table 2. Comparison between the Theoretical and Experimental Results for the glazing surface temperature and U-value using the calibrated hot box under different sets of controlled ambient temperature conditions.

Cond.	Text (°C)	Tint (°C)	Tint (Exp) (°C)	Text (Exp) (°C)	Tint (Theo) (°C)	Tint (Theo) (°C)	U-value total (Exp)	U-value total (Theo)
1	12.7	32.70	30.34	13.50	29.73	13.40	0.56	0.58
2	17.5	27.5	27.40	18.65	26.05	17.89	0.57	0.56
3	7.6	27.83	25.19	9.13	24.92	8.19	0.56	0.56

**Table 3.** Measured parameters and uncertainties

Parameters	Sensor	Uncertainties
Temperatures	K-type Thermocouples	$\pm 1.5\text{ }^\circ\text{C}$
Heat flux	Hukseflux Thermal Sensors	$\pm 1.9 \times 10^{-6}\text{ V/(W/m}^2\text{)}$
Solar radiation	Pyranometer	$\pm 5\%$
Maximum power produced by the PV VG-4L	RO4 with Keysight 34972A	Electric current (I) ( $\pm 1.5\text{ }\mu\text{A}$ ) Voltage (V) ( $\pm 190\text{ }\mu\text{V}$ )

**Performance Analysis under Real Conditions**

The developed mathematical model has been validated against indoor experimental analysis. Nonetheless, the true performance of the PV VG-4L under real sky conditions still needs to be investigated in order to further justify the validity of the mathematical model especially that the electrical performance of the thin film PV glazing could not be evaluated indoors. That said, this section first discusses the performance of the PV VG-4L under real conditions. To carry out the testing, the prototype was installed at E.ON 2016 research house at the University of Nottingham, United Kingdom with latitude of 52.9438° N, and longitude of -1.1934° W. It is important to note that the pyranometer to measure the incident solar radiation was placed parallel to the surface of the PV VG-4L. It is worth emphasising that the outdoor monitoring of the PV VG-4L has been conducted under two conditions; during the day and during the night (at zero solar radiation). The thermal and electrical characteristics of the PV VG-4L under real conditions were monitored using the sensors as summarised in Table 4. During the day, the reading given by the heat flux sensor for the thermal transmittance of the PV VG-4L gives the value of the heat

gain. Therefore, during the day, the only parameters that are being considered are the surface temperature difference of the PV VG-4L, its electrical power produced, and also the estimated g-factor. The typical monitoring period is between 9:30 a.m. to 5:00 p.m. in a typical day of June. Meanwhile, the focus of the experiment during the night is the thermal transmittance measurement or U-value. A 1kW convective heater was used as the heat source for indoors.

Figure 5 shows the solar radiation, surface temperatures of the PV VG-4L, and both internal and external; glazing surface temperature during the day and night. It should be noted that for the data taken on the 27<sup>th</sup> of June to 28<sup>th</sup> of June 2019, the average heating temperature was set to heat the ambient room at 24 to 25 °C. On the day of testing, the sky was in a clear sky condition and hence clear pattern of solar radiation curve with the time of the day was obtained. At low –zero solar radiation, the indoor surface temperature of the PV VG-4L is in general higher than its external surface temperature. However, as the incident solar radiation increases, the external surface temperature increases. The trend of the graph is explained as follows; when the PV component of the PV VG-4L absorbed the incident solar ra-

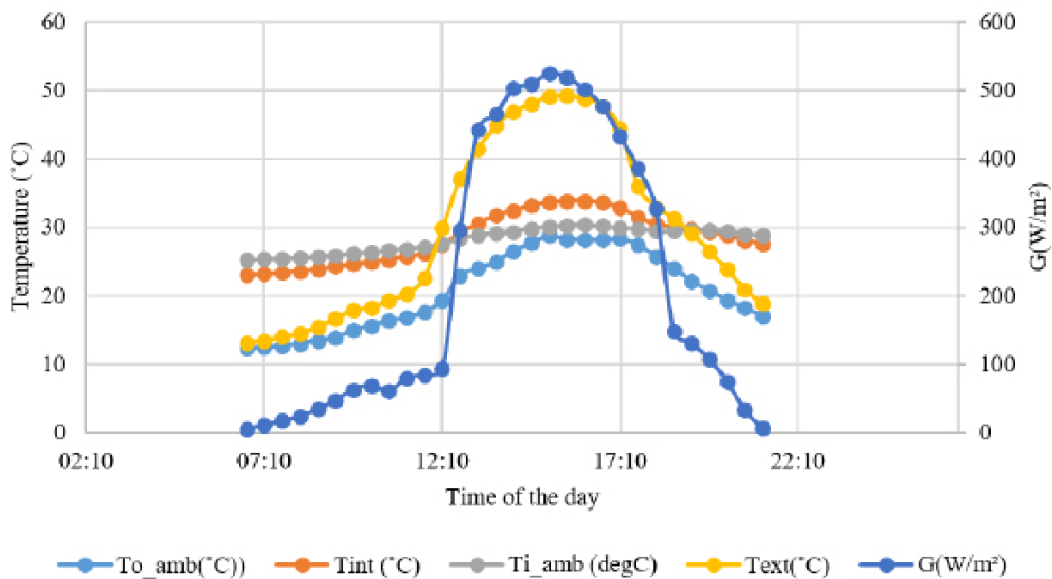


**Figure 5.** Variation in the external glazing surface temperature (Textl), internal glazing surface temperature (T\_int), Outdoor ambient temperature (To\_amb), indoor ambient temperature (Ti\_amb) and solar radiation with time of the day.

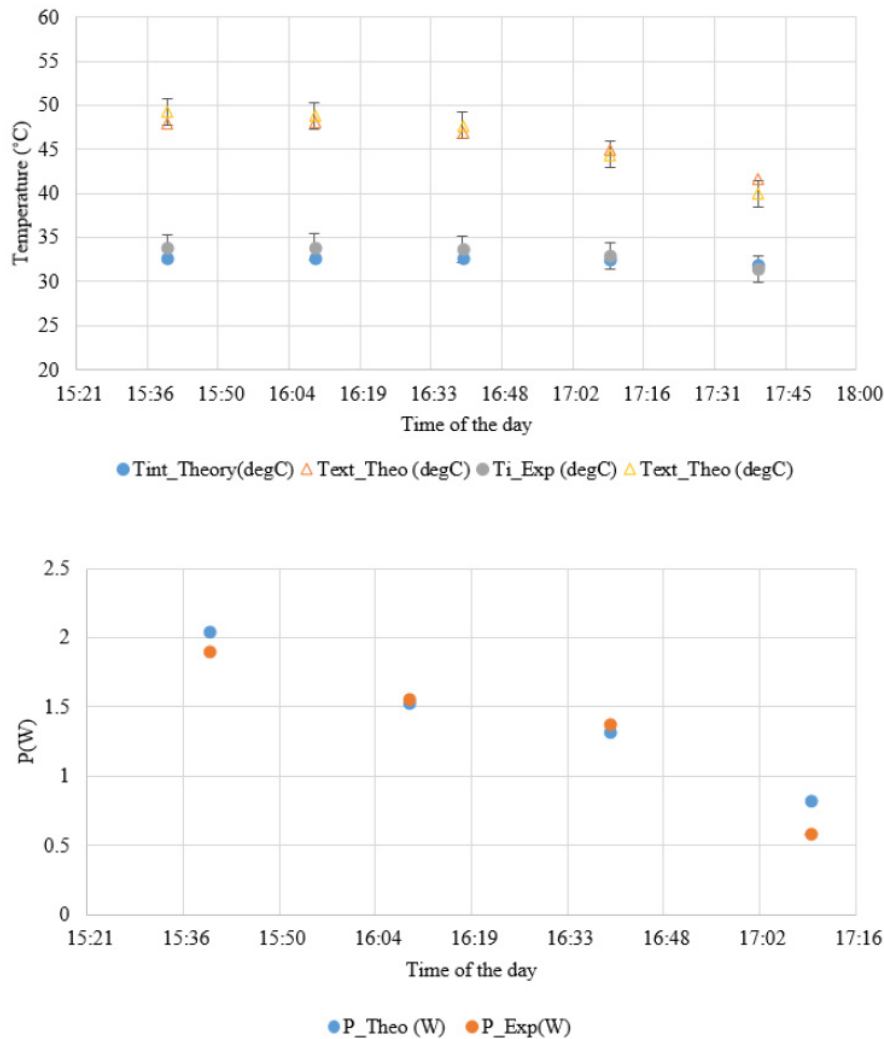


**Figure 6.** Top: Outdoor Experimental and Theoretical Curves for the Glazing surface temperatures (Tint) for the internal surface and (Text) for the external surface and bottom: Power produced per for 0.4 m x 0.4 m prototype as per time constant of the PV VG-4L with time of the day.

radiation, a fraction was converted into electrical energy meanwhile the rest was wasted in the form of heat. This heat act as the secondary heat source ( $q_2$ ) due to the PV element. However, the vacuum layer behind the PV component of the PV VG-4L act as the insulation layer or barrier to the heat flow of ( $q_2$ ) from being transferred indoors. As a result, the external surface temperature of the PV VG-4L became higher compared to its internal surface temperature, which is an advantage in the summer. For the data analysis, all the data was recorded for every 1 minute.

The outdoor experimental results as discussed previously, were compared with the theoretical results using the developed mathematical model. Due to the varying condition of the ambient climate, the electrical performance and thermal characteristics of PV VG-4L in a steady state condition are analysed as per time constant of the PV VG-4L. From our analysis, it is concluded that the computed time constant for the PV VG-4L is approximately 30 minutes.

The experimental results were compared based on the PV VG-4L surface temperature difference and electrical performance at quasi-steady state during the day and thermal transmittance or U-value during the night. Based on local weather data, the average wind speed during the day and night were approximated at 4.6 m/s and 3.5 m/s respectively. In the modelling, the dependency of the thermal and hence electrical performance of the PV VG-4L with the incident angle value which changes with the location and time of the day are being considered. The comparisons between the outdoor experimental and theoretical results are represented in Figure 6 and Figure 7 for the reading during the day and night respectively. The trend given by both outdoor experimental and theoretical curves are in good agreement. Figure 6 shows that the maximum power produced at average solar radiation of 500 W/m<sup>2</sup> is approximately 12 W/m<sup>2</sup> for 0.4 m x 0.4 m PV VG-4L made of amorphous silicon solar cells. It is worth emphasizing that, a different power produced is expected when a different type of thin film PV is

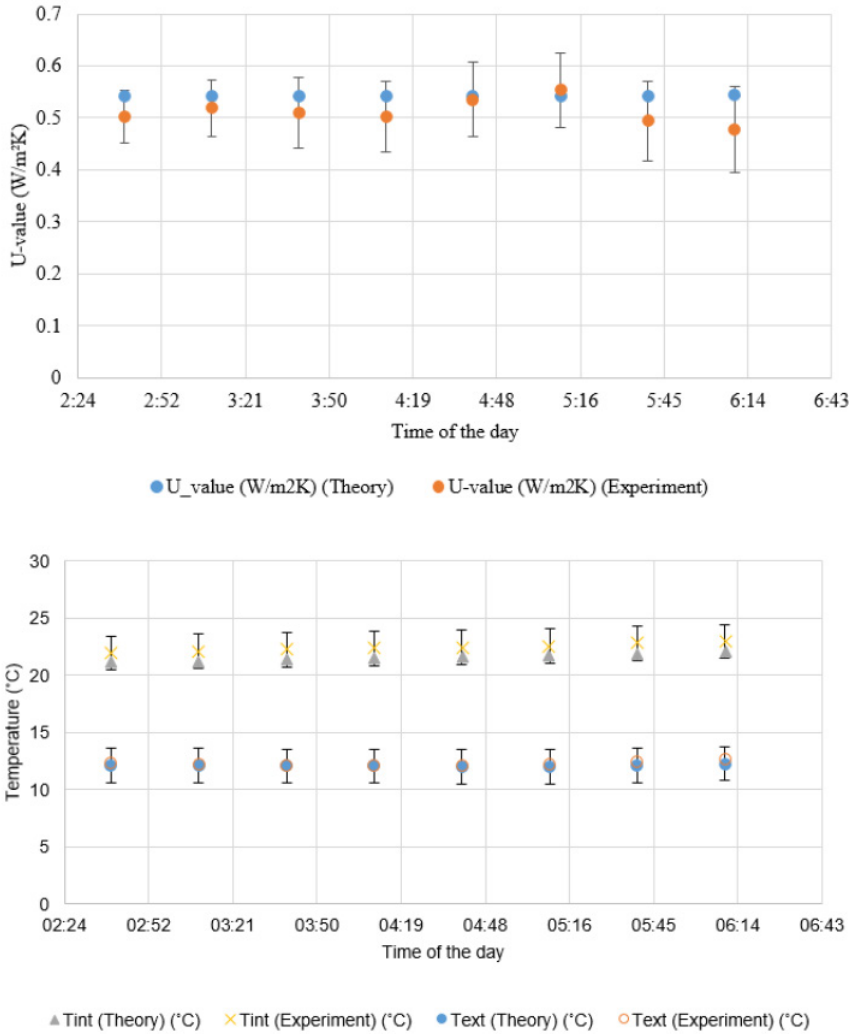


**Figure 7.** Top: Outdoor Experimental and Theoretical Curves for the Glazing surface temperature and bottom: U-value for 0.4 m x 0.4 m prototype as per time constant of the PV VG-4L with the time of the day (data was taken on the 27<sup>th</sup> of June 2019 at low-zero solar radiation).

used as the prototype. In order to further justify the validity of the mathematical model, error analysis using RMSPD analysis was performed. The average RMSPD for the glazing surface temperatures, the power produced and U-value are 2.58 %, 1.4% and 6.86 % respectively. It is worth noting that the derived absolute errors for the power produced are too small to be included in the plotted curves.

### Angle Dependence Solar Direct Transmittance

When the PV component of the PV VG-4L absorbed solar radiation, a fraction will be wasted in the form of heat which then reemitted or reradiated into the building internal space. This secondary heat source  $q_i$  factor when combined with the solar direct transmittance  $\tau_c$  the glazing will give us the solar heat gain coefficient or solar gain factor (g-value) given in equation (12).

$$g(\theta) = \tau_c(\theta) + q_i(\theta)$$

However, it is very important to emphasize that,  $\tau_c$  is solar angular dependence which means, the value will change according the sunny hours and hence the angle of the solar incidence  $\theta$  onto the PV VG-4L. Other than the solar heat gain coefficient,  $\tau_c$  is also important to compute

**Table 4.** The angular dependence solar direct transmittance  $\tau_c(\theta)$

The angle of solar incidence $\vartheta$	Angular dependence solar direct transmittance $\tau_c(\vartheta)$
0	22.0
10	21.8
20	21.6
30	21.3
40	21.1
50	19.6
60	18.7
70	15.1



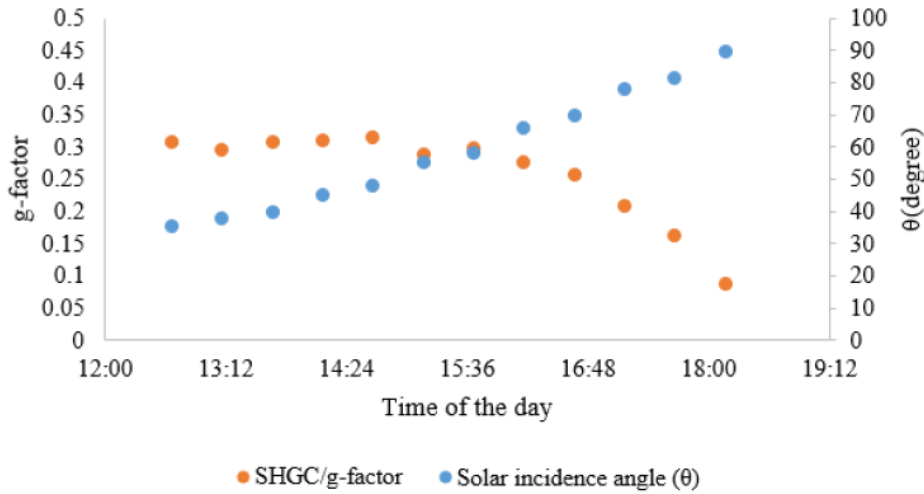


**Figure 8.** Obtained solar gain factor (g-factor) and the angle of incidence with time of the day.

the total amount of solar radiation absorbed by the different element of the PV VG-4L namely  $S_{g1}$ ,  $S_{g2}$ , and  $S_{TP}$ , in the above discussed mathematical model. Using the EDTM SS2450 solar spectrum meter [10], the normal incidence solar direct transmittance  $\tau_c(0)$  of the PV VG-4L was measured as 22%. However, due to the limited information on the angular dependence solar direct transmittance  $\tau_c(\theta)$ , the study conducted by [11] was being referred to estimate  $\tau_c(\theta)$  and the values summarised in Table 2.

In addition, the direct solar absorptance of the a-Si of PV VG-4L  $\alpha_e(\theta)$  which is given by  $1 - \tau_c(\theta) - \rho_e(\theta)$  where  $\rho_e(\theta)$  is the angular dependence reflectance is also assumed to follow the trend of the  $\tau_c(\theta)$ . This is because,  $\rho_e(\theta)$  increases with the increase in the angle of solar incidence, as concluded in [11]. Since we could measure  $q_i(\theta)$ , we could calculate  $g(\theta)$  that also changes with time of the day. At time when the solar incidence angle is low, high heat gain of approximately 30% was obtained, with  $\tau_c$  of 21.22%, the fraction of the solar energy absorbed by the PV module which is being re-emitted inside the building is almost 9%.

**Table 4.** The angular dependence solar direct transmittance  $\tau_c(\theta)$

The angle of solar incidence $\theta$	Angular dependence solar direct transmittance $\tau_c(\theta)$
0	22.0
10	21.8
20	21.6
30	21.3
40	21.1
50	19.6
60	18.7
70	15.1

### Building Thermal Load Calculation using a Simplified Energy Balance

With the validated mathematical model, building heating load performance when retrofitted with and without PV VG-4L based on the model of the Nottingham H.O.U.S.E [12] was calculated and compared. The calculation method used in this study is based on ISO 52016-1:2017 standards [13]. In general, the energy need by the building is calculated by using the energy balance quasi-steady-method as in equation (1). The total heat load of a building  $Q_{load}$  can be calculated by considering the total heat gains for the heating mode  $Q_{gain}$  hourly and the gain utilization factor:

$$Q_{load} = Q_{loss} - \eta_{utilisation} Q_{gain} \quad (13)$$

In any building, the heat loss from the building happened via heat transmission through external walls, top roof, the floor of the ground floor, windows and doors. The following equation represents the general equation to calculate the heat loss from a building:

$$Q_{loss} = U_{cH} \cdot A_{cH} (T_{indoor} - T_{ambient}) + Q_v \quad (14)$$

**Table 5.** Component of the house and the associated U-Value and Area.

Component	U-Value (W/m <sup>2</sup> )	Area (m <sup>2</sup> )
<i>Window</i>		
PV_SG	4.67	
PV_DG	2.8	25.83
PV_VG	0.60	
<i>Block wall</i>		
Floor	0.1	153.59
Roof	0.1	53.30
Skylight	0.13	54.50
Door	0.46	3.90
Door	0.16	2.08

of which,  $Q_v$  is the ventilation heat loss,  $U_{ch}$  and  $A_{ch}$  are the heat lost coefficient and surface area of the component of the house summarized as in Table 6 [12]:

Meanwhile, the total heat gain  $Q_g$  of the house is calculate by considering both solar heat gain  $Q_{SHG}$  from the glazing component of the house and also the internal heat gain  $Q_{IHG}$ . The total solar heat gain  $Q_{SHG}$  is calculated using the following equation

$$Q_{SHG} = SHGC \times (G_{\text{global solar radiation}}) \quad (15)$$

Meanwhile, to calculate  $Q_{IHG}$ , the following assumptions are considered; i) There are two occupants in the house, ii) all equipment were assumed to be energy efficient and iii) lighting was assumed to be provided by low-energy com-

pact florescent bulbs. The important values in regard to the latent and sensible heat generated by the spaces in the house are summarised in Table 6 [12], :

Equation 5.25 from page 5-17 of Guide A: Environmental Design – CIBSE [14] is being referred to calculate  $Q_{IHG}$  and hence the following equation was developed in this study:

$$Q_{IHG} = (Q_{\text{kitchen}} \times t_{\text{kitchen}} + Q_{\text{diningroom}} \times t_{\text{diningroom}} + Q_{\text{livingroom}} \times t_{\text{livingroom}} + Q_{\text{bedrooms}} \times t_{\text{bedrooms}} + Q_{\text{circulation}} \times t_{\text{circulation}} + Q_{\text{toilet}} \times t_{\text{toilet}} + Q_{\text{people}} \times t_{\text{people}}) \times \frac{1}{24} \quad (16)$$

**Table 6.** Important values in regard to the latent and sensible heat generated by the spaces in the house.

Space	Sensible heat (W/m <sup>2</sup> )	Latent heat (W/m <sup>2</sup> )	Average sensible equipment gained (W/m <sup>2</sup> )	Thermal loads due to lighting (W/m <sup>2</sup> )
Kitchen	3.8	1.9	0.5	0.5
Dining room	5.2	2.6	0.5	0.5
Living room	5.0	2.5	0.6	0.6
Bedrooms	4.9	2.4	0.25	0.25
Circulation	1	0.5	0.25	0.25
Toilet and bathroom	1.9	0.95	0.15	0.15

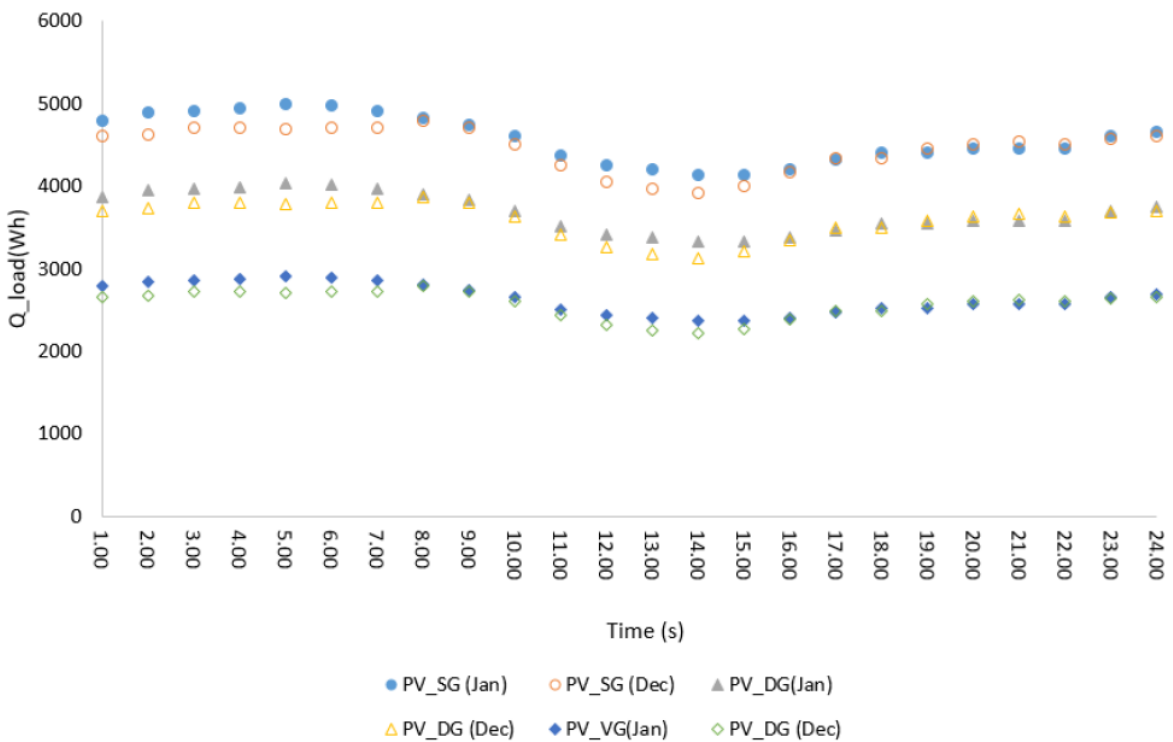


**Figure 9.** Predicted hourly averaged heat load in January for the a-Si (40%) type thin film PV glazing on its own (PV\_SG), in double glazing (PV\_DG) and vacuum glazing (PV\_VG).

The energy balance equations developed to calculate the total heat load were written in MATLAB to compute the results. As shown in the figures below are the hourly average analysis of the heat load from December to March, for Nottingham, UK weather data. From the analysis, one can estimate the amount of the heat load when the thin film PV glazing installed on its own (PV\_SG), with double glazing (PV\_DG) and with vacuum glazing (PV VG-4L). The analysis was explicitly analyzed into two time windows. The first is from 10:00 a.m. to 4:00 p.m. and the second is from 4:00 p.m. to 10:00 a.m. where the SHCG is assumed negligible.

Based on the model of the Nottingham H.O.U.S.E, the building heat load was modelled, and the carbon emission was estimated. In comparison to the thin film PV glazing on its own i.e. PV\_SG, the reduction in the amount of the building heat load by almost 50% is possible with the use of vacuum glazing (PV\_VG). It is worth noting that, the PV\_VG can generate power for the LED, florescent lights and appliances installed in the building. In addition, unlike conventional opaque PV panels. PV-vacuum glazing allows day lighting.

## CONCLUSION

An integrated semi-transparent thin film photovoltaic glazing with vacuum insulated layer (PV VG-4L) is presented in this paper. A mathematical model was developed by taking into account all the parameters related to the individual component of a typical vacuum glazing unit which is the dominant in the design and also the fraction the solar radiation absorbed by the different layers of PV VG-4L. To validate the mathematical model, a lab-scale prototype was manufactured and tested indoors using a calibrated hot box, and outdoors by installing the sample at a research house. From the indoor analysis, the computed RMSPD value for the glazing surface temperature and the U-value are 4.75 % and 0.96% respectively. Meanwhile, when investigated under real conditions (field testing), the RMPSD computed for the glazing surface temperatures, electrical power generated under real conditions and U-value are 2.58 %, 1.4% and 6.86 % respectively. The validated mathematical model would allow us to further carry out optimisation and performance analysis of the PV VG-4L under various environmental condition which will be explored in the future. Under controlled conditions, by following closely the ISO 12567 standards, the overall U-value of the PV VG-4L was measured to be as low as 0.6 W/m<sup>2</sup>K. When investigated under real conditions, an obvious trend in glazing surface temperature variation with solar radiation was obtained. During low to zero solar radiation, the internal glazing surface temperature is on average higher in comparison to the external glazing surface temperature. However, as the

solar radiation increases, the by-product of the absorbed heat by the thin film PV glazing layer, has led to the increase in the external glazing surface temperature as the heat transfer from the secondary heat source to internal surface is reduced by the vacuum layer. Nevertheless, the heat gain into the internal building or space area was still measurable due to the solar transmittance of the PV VG-4L. At average solar radiation of 500 W/m<sup>2</sup>, the PV VG-4L can in total of 12 W of power per m<sup>2</sup> of panel. Meanwhile, as shown in Figure 7, at low to zero solar radiation (i.e. during the night), at outdoor ambient temperature of 14°C, the average U-value of the typical PV VG-4L was found to be as low as 0.54 W/m<sup>2</sup>K. For a conventional thin film PV glazing, to improve the thermal performance of the thin film PV glazing, a combination with a double-glazing unit is possible with the estimated U-value of 2.5-2.8 W/m<sup>2</sup>K depending on the type of gas used to provide the insulation in the air gap. Clearly, the vacuum layer introduced in the PV VG-4L design presented in this paper is better in performance with the slim configuration of the glazing unit as an additional benefit. The results also show that the PV VG-4L not only can produce power but also has high insulation properties when compared to a single thin film PV glazing with a typical U-value of approximately 5 W/m<sup>2</sup>K; the U-value is higher by almost 90%. The promising U-value implies its range of potential applications can be improved depending on the energy needs and applications, such as for BIPV solar façade (PV curtain walling) in commercial buildings, greenhouses, skylight and conservatory.

## ACKNOWLEDGEMENT

The authors gratefully acknowledge Innovate UK's financial support through Newton Fund (Project reference no: 102882) and International Science & Technology Cooperation Program of China (No. 2016YFE0124300).

---

## References

---

1. IEA. Buildings Tracking Clean Energy Progress 2019; Available from: <https://www.iea.org/tcep/buildings/>.
2. Markets, R.a. \$7 Bn Building Integrated Photovoltaics (BIPV) Market - Global Outlook and Forecast 2019-2024. 2019 [cited 2019 14 October]; Available from: <https://www.globenewswire.com/news-release/2019/02/08/1713914/0/en/7-Bn-Building-Integrated-Photovoltaics-BIPV-Market-Global-Outlook-and-Forecast-2019-2024.html>.
3. Martin-Chivelet, N., et al., Comparative Performance of Semi-Transparent PV Modules and Electrochromic Windows for Improving Energy Efficiency in Buildings. *Energies*, 2018. 11(6): p. 1526.
4. Liu, H.-M., et al., Improving the Performance of a Semitransparent BIPV by Using High-Reflectivity Heat Insulation Film. *International Journal of Photoenergy*, 2016. 2016: p. 15.
5. Zhang, W., L. Lu, and X. Chen, Performance Evaluation of

- Vacuum Photovoltaic Insulated Glass Unit. *Energy Procedia*, 2017. 105(Supplement C): p. 322-326.
6. Ghosh, A., S. Sundaram, and T.K. Mallick, Investigation of thermal and electrical performances of a combined semi-transparent PV-vacuum glazing. *Applied Energy*, 2018. 228: p. 1591-1600.
  7. Schott, T. Operational temperatures of PV modules. in 6th PV solar energy conference. 1985.
  8. Evans, D., Simplified method for predicting PV array output. *Solar Energy*, 1981. 27: p. 555–560.
  9. JARIMI, H., et al. An affordable small calibrated hot box suitable for thermal performance measurement of a glazing unit. in 17th International Conference on Sustainable Energy Technologies 21st to 23rd August 2018. 2018. Wuhan, China.
  10. EDTM. EDTM SS2450 | Solar Spectrum Meter. 2019 [cited 2019 14 July 2019]; Available from: <https://www.edtm.com/index.php/ss2450-solar-spectrum-meter>.
  11. Moralejo Vázquez, F.J.a.M.C., Nuria and Olivieri, Lorenzo and Caamaño Martín, Estefanía Optical characterisation of semi-transparent PV modules for building integration., in 29th European Photovoltaic Solar Energy Conference and Exhibition (EU PVSEC 2014). 2014: Amsterdam, The Netherlands. . p. 1-9.
  12. Liu, L., Investigation on solar/thermoelectric collector for building application, in Department of Architecture and Built Environment. 2014, University of Nottingham: UK.
  13. Bsi, BS EN ISO 52016-1:2017 Energy performance of buildings. Energy needs for heating and cooling, internal temperatures and sensible and latent heat loads. Calculation procedures. 2017.
  14. CIBSE, GVA/15 CIBSE Guide A: Environmental Design 2015. 2015: CIBSE. 402.